

Role of defects and disorder in the half-metallic full-Heusler compounds

Iosif Galanakis¹, Kemal Özdoğan², and Ersoy Şaşıoğlu^{3,4}

¹ Department of Materials Science, School of Natural Sciences, University of Patras, GR-26504 Patra, Greece

² Department of Physics, Gebze Institute of Technology, Gebze, 41400, Kocaeli, Turkey

³ Institut für Festkörperforschung, Forschungszentrum Jülich, D-52425 Jülich, Germany

⁴ Fatih University, Physics Department, 34500, Büyükçekmece, İstanbul, Turkey

Emails: galanakis@upatras.gr, kozdogan@gyte.edu.tr, e.sasioglu@fz-juelich.de

Summary. Half-metallic ferromagnets and especially the full-Heusler alloys containing Co are at the center of scientific research due to their potential applications in spintronics. For realistic devices it is important to control accurately the creation of defects in these alloys. We review some of our late results on the role of defects and impurities in these compounds. More precisely we present results for the following cases (i) doping and disorder in $\text{Co}_2\text{Cr}(\text{Mn})\text{Al}(\text{Si})$ alloys, (ii) half-metallic ferrimagnetism appeared due to the creation of $\text{Cr}(\text{Mn})$ antisites in these alloys, (iii) Co-doping in $\text{Mn}_2\text{VAl}(\text{Si})$ alloys leading to half-metallic antiferromagnetism, and finally (iv) the occurrence of vacancies in the full-Heusler alloys containing Co and Mn. These results are susceptible of encouraging further theoretical and experimental research in the properties of these compounds.

1 Introduction

Heusler alloys [1] have attracted during the last century a great interest due to the possibility to study in the same family of alloys a series of interesting diverse magnetic phenomena like itinerant and localized magnetism, antiferromagnetism, helimagnetism etc [2, 3, 4, 5, 6, 7]. The first Heusler alloys studied were crystallizing in the $L2_1$ structure which consists of 4 fcc sublattices. Afterwards, it was discovered that it is possible to leave one of the four sublattices unoccupied ($C1_b$ structure). The latter compounds are often called half- or semi-Heusler alloys, while the $L2_1$ compounds are referred to as full-Heusler alloys. NiMnSb belongs to the half-Heusler alloys [8]. In 1983 de Groot and his collaborators [9] showed by using first-principles electronic structure calculations that this compound is in reality half-metallic, i.e. the minority band is semiconducting with a gap at the Fermi level E_F , leading to 100% spin polarization at E_F . Other known half-metallic materials except the half- and full-Heusler alloys (see [10, 11, 12, 13] and references therein) are

some oxides (*e.g.* CrO_2 and Fe_3O_4) [14], the manganites (*e.g.* $\text{La}_{0.7}\text{Sr}_{0.3}\text{MnO}_3$) [14], the double perovskites (*e.g.* $\text{Sr}_2\text{FeReO}_6$) [15], the pyrites (*e.g.* CoS_2) [16], the transition metal chalcogenides (*e.g.* CrSe) and pnictides (*e.g.* CrAs) in the zinc-blende or wurtzite structures [17, 18, 19, 20, 21, 22, 23, 24, 25, 26, 27, 28, 29, 30, 31, 32, 33, 34, 35, 36, 37, 38, 39, 40, 41], the europium chalcogenides (*e.g.* EuS) [42] and the diluted magnetic semiconductors (*e.g.* Mn impurities in Si or GaAs) [43, 44]. Although thin films of CrO_2 and $\text{La}_{0.7}\text{Sr}_{0.3}\text{MnO}_3$ have been verified to present practically 100% spin-polarization at the Fermi level at low temperatures [14, 45], the Heusler alloys remain attractive for technical applications like spin-injection devices [46], spin-filters [47], tunnel junctions [48], or GMR devices [49, 50] due to their relatively high Curie temperature compared to these compounds [2].

Ishida and collaborators studied by means of *ab-initio* calculations the full-Heusler compounds of the type Co_2MnZ , where Z stands for Si and Ge, and have shown that they are half-metals [51]. Later the origin of half-metallicity in these compounds has been largely explained [52]. Many experimental groups during the last years have worked on these compounds and have tried to synthesize them mainly in the form of thin films and incorporate them in spintronic devices. The group of Westerholt has extensively studied the properties of Co_2MnGe films and they have incorporated this alloy in the case of spin-valves and multilayer structures [53, 54, 55]. The group of Reiss managed to create magnetic tunnel junctions based on Co_2MnSi [56, 57]. A similar study of Sakuraba and collaborators resulted in the fabrication of magnetic tunnel junctions using Co_2MnSi as one magnetic electrode and Al-O as the barrier ($\text{Co}_{75}\text{Fe}_{25}$ is the other magnetic electrode) and their results are consistent with the presence of half-metallicity for Co_2MnSi [58]. Dong and collaborators recently managed to inject spin-polarized current from Co_2MnGe into a semiconducting structure [59]. Finally Kallmayer *et al.* studied the effect of substituting Fe for Mn in Co_2MnSi films and have shown that the experimental extracted magnetic spin moments are compatible with the half-metallicity for small degrees of doping [60].

It is obvious from the experimental results that the full-Heusler compounds containing Co and Mn are of particular interest for spintronics. Not only they combine high Curie temperatures and coherent growth on top of semiconductors (they consist of four fcc sublattice with each one occupied by a single chemical element) but in real experimental situations they can preserve a high degree of spin-polarization at the Fermi level. In order to accurately control their properties it is imperative to investigate the effect of defects, doping and disorder on their properties. Recently Picozzi *et al.* published a study on the effect of defects in Co_2MnSi and Co_2MnGe [61] followed by an extensive review of the defects in these alloys [62].

Authors have studied in the recent years several aspects of these half-metallic alloys like the origin of the gap [52, 63], properties of surfaces [64, 65, 66] and interfaces with semiconductors [67, 68], the quaternary

[69, 70], the orbital magnetism [71, 72], the exchange constants [73], the magneto-optical properties [74], the half-metallic ferrimagnetic Heusler alloys like Mn_2VAl , [75, 76] and the fully-compensated half-metallic ferrimagnets or simply half-metallic antiferromagnets [77]. In this chapter we will overview some of our results on the defects in the half-metallic full Heusler alloys obtained using the full-potential nonorthogonal local-orbital minimum-basis band structure scheme (FPLO) [78, 79] within the local density approximation (LDA) [80, 81, 82] and employing the coherent potential approximation (CPA) to simulate the disorder in a random way [79]. In section 2 we present the physics of defects in the ferromagnetic Heusler alloys containing Co and Mn like Co_2MnSi [83, 84]. In section 3 we show the creation of half-metallic ferrimagnets based on the creation of Cr and Mn antisites in $\text{Co}_2(\text{Cr}$ or $\text{Mn})(\text{Al}$ or $\text{Si})$ alloys [85, 86] and in section 4 we expand this study to cover the case of Co defects in ferrimagnetic Mn_2VAl and Mn_2VSi alloys leading to half-metallic antiferromagnets [87]. In section 5 we investigate a special case: the occurrence of vacancies in the full-Heusler compounds [88]. Finally in section 6 we summarize and conclude.

2 Defects in full-Heuslers containing Co and Mn

We will start our discussion presenting our results on the defects in the case of Co_2MnZ alloys where Z is Al and Si [83, 84]. The first part of our investigation in this section concerns the doping of Co_2MnSi . To simulate the doping by electrons we substitute Fe for Mn while to simulate the doping of the alloys with holes we substitute Cr for Mn. We have studied the cases of moderate doping substituting 5%, 10% and 20% of the Mn atoms. We will start our discussion from figure 1 where we present the total density of states (DOS) for the $\text{Co}_2[\text{Mn}_{1-x}\text{Fe}_x]\text{Si}$ and $\text{Co}_2[\text{Mn}_{1-x}\text{Cr}_x]\text{Si}$ compounds. As discussed in reference [52] the gap is created between states located exclusively at the Co sites. The states low in energy (around -6 eV) originate from the low-lying *p*-states of the *sp* atoms (there is also an *s*-type state very low in energy which is not shown in the figure). The majority-spin occupied states form a common Mn-Co band while the occupied minority states are mainly located at the Co sites and the minority unoccupied states at the Mn sites. Doping the perfect ordered alloy with either Fe or Cr smoothenes the valleys and peaks along the energy axis. This is a clear sign of the chemical disorder; Fe and Cr induce peaks at slightly different places than the Mn atoms resulting to this smoothening and as the doping increases this phenomenon becomes more intense. The important detail is what happens around the Fermi level and in what extent is the gap in the minority band affected by the doping. So now we will concentrate only at the enlarged regions around the Fermi level. The blue dashed lines represent the Cr-doping while the red dash-dotted lines are the Fe-doped alloys. Cr-doping has only marginal effects to the gap. Its width is narrower with respect to the perfect compounds

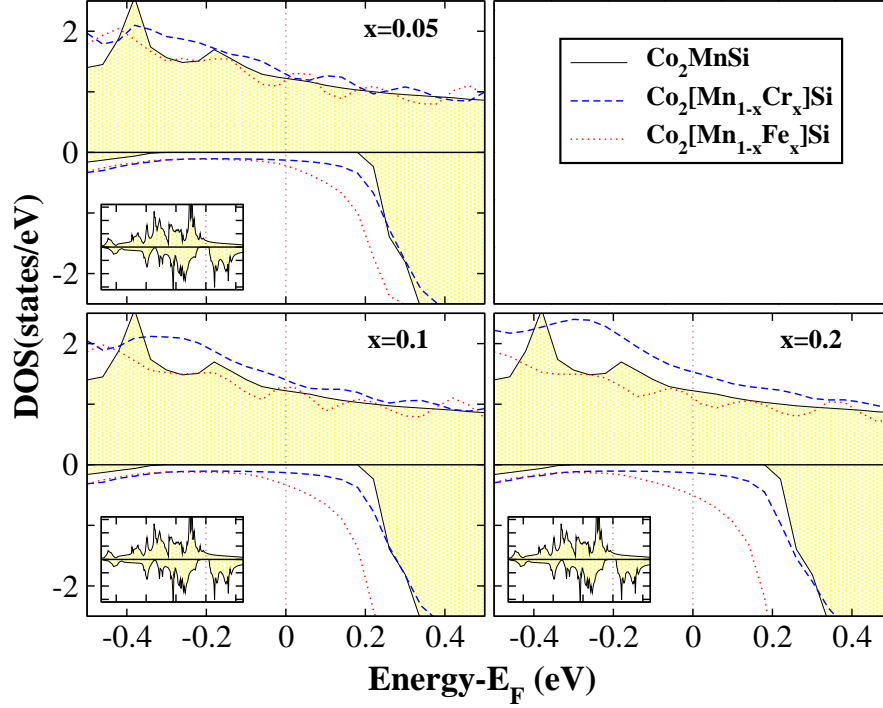


Fig. 1. (Color online) Spin-resolved total density of states (DOS) for the case of $\text{Co}_2[\text{Mn}_{1-x}\text{Cr}_x]\text{Si}$ and $\text{Co}_2[\text{Mn}_{1-x}\text{Fe}_x]\text{Si}$ for three difference values of the doping concentration x . DOS's are compared to the one of the undoped Co_2MnSi alloy. In the insets we present the DOS for a wider energy range. We have set the Fermi level as the zero of the Energy axis. Note that positive values of DOS refer to the majority-spin electrons and negative values to the minority-spin electrons.

but overall the compounds retain their half-metallicity. In the case of Fe-doping the situation is more complex. Adding electrons to the system means that, in order to retain the perfect half-metallicity, these electrons should occupy high-energy lying antibonding majority states. This is energetically not very favorable and for these moderate degrees of doping a new shoulder appears in the unoccupied states which is close to the right-edge of the gap; a sign of a large change in the competition between the exchange splitting of the Mn majority and minority states and of the Coulomb repulsion. In the case of the 20% Fe doping this new peak crosses the Fermi level and the Fermi level is no more exactly in the gap but slightly above it. Further substitution should lead to the complete destruction of the half-metallicity as in the Quaternary Heusler alloys with a Mn-Fe disordered site [89]. Recent ab-initio calculations including the on-site Coulomb repulsion (the so-called Hubbard U) have predicted that Co_2FeSi is in reality half-metallic reaching a

total spin magnetic moment of $6 \mu_B$ which is the largest known spin moment for a half-metal [90, 91].

We expand our theoretical work to include also the case of Co_2MnAl compound which has one valence electron less than Co_2MnSi . The extra electron in the the latter alloy occupies majority states leading to an increase of the exchange splitting between the occupied majority and the unoccupied minority states and thus to larger gap-width for the Si-based compound. In the case of Al-based alloy the bonding and antibonding minority d-hybrids almost overlap and the gap is substituted by a region of very small minority density of states (DOS); we will call it a pseudogap. In both cases the Fermi level falls within the gap (Co_2MnSi) or the pseudogap (Co_2MnAl) and an almost perfect spin-polarization at the Fermi level is preserved.

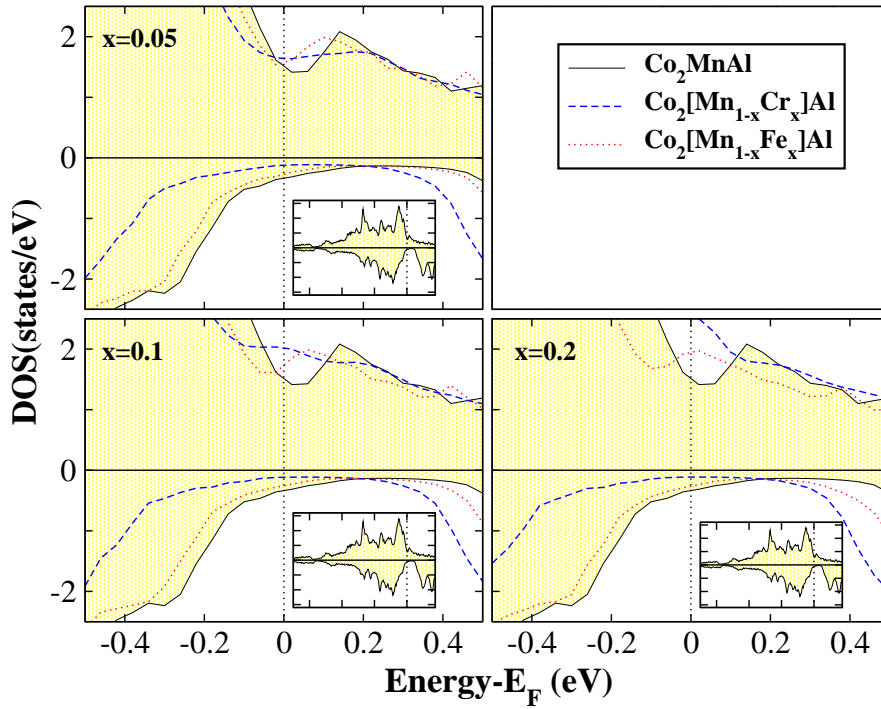


Fig. 2. (Color online) Spin-resolved DOS for the case of $\text{Co}_2[\text{Mn}_{1-x}\text{Cr}_x]\text{Al}$ and $\text{Co}_2[\text{Mn}_{1-x}\text{Fe}_x]\text{Al}$ for three values of the doping concentration x . DOS's are compared to the one of the undoped Co_2MnAl alloy. Details as in figure 1.

We substitute either Fe or Cr for Mn to simulate the doping by electrons and holes, respectively, in Co_2MnAl . In figure 2 we present the total density of states (DOS) for the $\text{Co}_2[\text{Mn}_{1-x}(\text{Fe or Cr})_x]\text{Al}$ alloys to compare to the perfect Co_2MnAl alloys. As was the case also for the compounds in reference

[83] and discussed above the majority-spin occupied states form a common Mn-Co band while the occupied minority states are mainly located at the Co sites and minority unoccupied at the Mn sites (note that the minority unoccupied states near the gap are Co-like but overall the Mn-weight is dominant). The situation is reversed with respect to the Co_2MnSi compound and Cr-doping has significant effects on the pseudogap. Its width is larger with respect to the perfect compound and becomes slightly narrower as the degree of the doping increases. Fe-doping on the other hand almost does not change the DOS around the Fermi level. The extra-electrons occupy high-energy lying antibonding majority states but since Co_2MnAl has one valence electron less than Co_2MnSi half-metallicity remains energetically favorable and no important changes occur upon Fe-doping and further substitution of Fe for Mn should retain the half-metallicity even for the Co_2FeAl compound although LDA-based ab-initio calculations predict that the limiting case of Co_2FeAl is almost half-metallic [89].

Table 1. Total and atom-resolved spin magnetic moments for the case of excess of Mn (x positive) or sp atoms (x negative) atoms in μ_B . The spin moments have been scaled to one atom. In the second column the ideal total spin moment if the compound was half-metallic.

		$\text{Co}_2\text{Mn}_{1+x}\text{Al}_{1-x}$			
x	Ideal	Total	Co	Mn	Al
-0.20	3.40	3.26	1.09	2.89	-0.12
-0.10	3.70	3.64	1.22	2.84	-0.13
-0.05	3.85	3.83	1.29	2.83	-0.13
0.00	4.00	4.04	1.36	2.82	-0.14
0.05	4.15	4.22	1.40	2.81	-0.14
0.10	4.30	4.40	1.44	2.81	-0.14
0.20	4.60	4.80	1.54	2.81	-0.15
		$\text{Co}_2\text{Mn}_{1+x}\text{Si}_{1-x}$			
x	Ideal	Total	Co	Mn	Al
-0.20	4.40	4.40	1.92	3.19	-0.06
-0.10	4.70	4.70	1.95	3.15	-0.08
-0.05	4.85	4.85	1.96	3.14	-0.08
0.00	5.00	5.00	1.96	3.13	-0.09
0.05	5.15	5.15	1.99	3.10	-0.10
0.10	5.30	5.30	2.00	3.09	-0.10
0.20	5.60	5.60	2.03	3.05	-0.11

Finally we shall briefly discuss the case of disorder simulated by the excess of the Mn or the sp atoms. In table 1 we have gathered the total and atomic spin moments for all cases under study. Substituting 5%, 10%, 15% or 20% of the Mn atoms by Al or Si ones, corresponding to the negative values of x in the table, results in a decrease of 0.15, 0.30, 0.45 and 0.60 of the total

number of valence electrons in the cell, while the inverse procedure results to a similar increase of the mean value of the number of valence electrons. Contrary to the Si compound which retains the perfect half-metallicity, the Al-based compound is no more half-metallic. In the case of Co_2MnSi disorder induces states at the edges of the gap keeping the half-metallic character but this is no more the case for Co_2MnAl compound where no real gap exists [83, 84].

3 Defects driven half-metallic ferrimagnetism

In the previous section we have examined the case of defects in half-metallic ferromagnets. But the ideal case for applications would be a half-metallic antiferromagnet (HMA), also known as fully-compensated ferrimagnet [92], since such a compound would not give rise to stray flux and thus would lead to smaller energy consumption in devices. Also half-metallic ferrimagnetism (HMF_i) is highly desirable in the absence of HMA since such compounds would yield lower total spin moments than the corresponding ferromagnets. Well-known HMF_i are the perfect Heusler compounds FeMnSb and Mn_2VAl [93]. We will present in this section another route to half-metallic ferrimagnetism based on antisites created by the migration of Cr(Mn) atoms at Co sites in the case of Co_2CrAl , Co_2CrSi , Co_2MnAl and Co_2MnSi alloys.

We will start our discussion from the Cr-based alloys and using Co_2CrAl and Co_2CrSi as parent compounds we create a surplus of Cr atoms which sit at the perfect Co sites. In figure 3 we present the total density of states (DOS) for the $[\text{Co}_{1-x}\text{Cr}_x]_2\text{CrAl}$ and $[\text{Co}_{1-x}\text{Cr}_x]_2\text{CrSi}$ alloys for concentrations $x=0$ and 0.1 , and in table 2 we have gathered the spin moments for the two compounds under study. We will start our discussion from the DOS. The perfect compounds show a gap in the minority-spin band and the Fermi level falls within this gap and thus the compounds are half-metals. When the sp atom is Si instead of Al the gap is larger due to the extra electron which occupies majority states of the transition metal atoms [52] and increases the exchange splitting between the majority occupied and the minority unoccupied states. This electron increases the Cr spin moment by $\sim 0.5 \mu_B$ and the moment of each Co atom by $\sim 0.25 \mu_B$ about. The Cr and Co majority states form a common band and the weight at the Fermi level is mainly of Cr character. The minority occupied states are mainly of Co character. When we substitute Cr for Co, the effect on the atomic DOS of the Co and Cr atoms at the perfect sites is marginal. The DOS of the impurity Cr atoms has a completely different form from the Cr atoms at the perfect sites due to the different symmetry of the site where they sit. But although Cr impurity atoms at the antisites induce minority states within the gap, there is still a tiny gap and the Fermi level falls within this gap keeping the half-metallic character of the parent compounds even when we substitute 20% of the Co atoms by Cr ones.

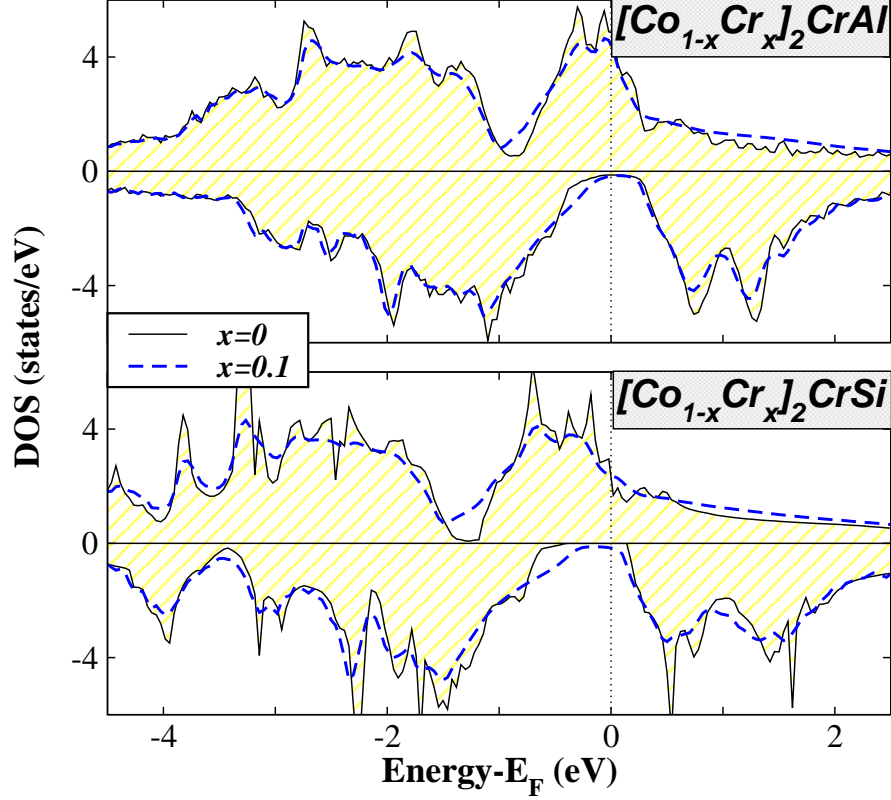


Fig. 3. (Color online) Total density of states (DOS) as a function of the concentration x for the $[\text{Co}_{1-x}\text{Cr}_x]_2\text{CrAl}$ (upper panel) and $[\text{Co}_{1-x}\text{Cr}_x]_2\text{CrSi}$ (lower panel) compounds.

The discussion above on the conservation of the half-metallicity is confirmed when we compare the calculated total moments in table 2 with the values predicted by the Slater Pauling rule for the ideal half-metals (the total spin moment in μ_B is the number of valence electrons in the unit cell minus 24) [52]. Since Cr is lighter than Co, substitution of Cr for Co decreases the total number of valence electrons and the total spin moment should also decrease. The interesting point is the way that the reduction of the total spin moment is achieved. Co and Cr atoms at the perfect sites show a small variation of their spin magnetic moments with the creation of defects and the total spin moment is reduced due to the antiferromagnetic coupling between the Cr impurity atoms and the Co and Cr ones at the ideal sites, which would have an important negative contribution to the total moment as confirmed by the results in table 2. Thus the Cr-doped alloys are half-metallic ferrimagnets and their total spin moment is considerable smaller than the perfect half-

Table 2. Atom-resolved spin magnetic moments for the $[\text{Co}_{1-x}\text{Cr}_x]_2\text{CrAl}$, $[\text{Co}_{1-x}\text{Cr}_x]_2\text{CrSi}$, $[\text{Co}_{1-x}\text{Mn}_x]_2\text{MnAl}$ and $[\text{Co}_{1-x}\text{Mn}_x]_2\text{MnSi}$ compounds (moments have been scaled to one atom). The two last columns are the total spin moment (Total) in the unit cell calculated as $2 \times [(1-x) * m^{\text{Co}} + x * m^{\text{Cr or Mn(imp)}}] + m^{\text{Cr(Mn)}} + m^{\text{Al or Si}}$ and the ideal total spin moment predicted by the Slater-Pauling rule for half-metals (see reference [52]). With Cr(imp) or Mn(imp) we denote the Cr(Mn) atoms sitting at perfect Co sites.

$[\text{Co}_{1-x}\text{Cr}_x]_2\text{CrAl}$							
x	Co	Cr(imp)	Cr	Al	Total	Ideal	
0	0.73	–	1.63	-0.09	3.00	3.00	
0.05	0.71	-1.82	1.62	-0.09	2.70	2.70	
0.1	0.69	-1.85	1.61	-0.08	2.40	2.40	
0.2	0.64	-1.87	1.60	0.06	1.80	1.80	
$[\text{Co}_{1-x}\text{Cr}_x]_2\text{CrSi}$							
x	Co	Cr(imp)	Cr	Si	Total	Ideal	
0	0.95	–	2.17	-0.06	4.00	4.00	
0.05	0.93	-1.26	2.12	-0.06	3.70	3.70	
0.1	0.91	-1.26	2.07	-0.05	3.40	3.40	
0.2	0.87	-1.25	1.96	-0.04	2.80	2.80	
$[\text{Co}_{1-x}\text{Mn}_x]_2\text{MnAl}$							
x	Co	Mn(imp)	Mn	Al	Total	Ideal	
0	0.68	–	2.82	-0.14	4.04	4.00	
0.05	0.73	-2.59	2.82	-0.13	3.81	3.80	
0.1	0.78	-2.49	2.83	-0.12	3.61	3.60	
0.2	0.84	-2.23	2.85	-0.09	3.20	3.20	
$[\text{Co}_{1-x}\text{Mn}_x]_2\text{MnSi}$							
x	Co	Mn(imp)	Mn	Si	Total	Ideal	
0.0	0.98	–	3.13	-0.09	5.00	5.00	
0.05	0.99	-0.95	3.09	-0.08	4.80	4.80	
0.1	0.99	-0.84	3.06	-0.07	4.60	4.60	
0.2	0.97	-0.70	2.99	-0.05	4.20	4.20	

metallic ferromagnetic parent compounds; in the case of $[\text{Co}_{0.8}\text{Cr}_{0.2}]_2\text{CrAl}$ it decreases down to $1.8 \mu_B$ from the $3 \mu_B$ of the perfect Co_2CrAl alloy. Here we have to mention that if also Co atoms migrate to Cr sites (case of atomic swaps) the half-metallity is lost, as it was shown by Miura et al. [94], due to the energy position of the Co states which have migrated at Cr sites.

In the rest of this section we will present results on the $[\text{Co}_{1-x}\text{Mn}_x]_2\text{MnZ}$ compounds varying the sp atom, Z, which is one of Al or Si. We have taken into account five different values for the concentration x ; $x=0, 0.025, 0.05, 0.1, 0.2$. In figure 4 we have drawn the total density of states (DOS) for both families of compounds under study and for two different values of the concentration x : the perfect compounds ($x=0$) and for one case with defects, $x=0.1$. In the case of the perfect Co_2MnSi compound there is a real gap in the minority spin band and the Fermi level falls within this gap and this

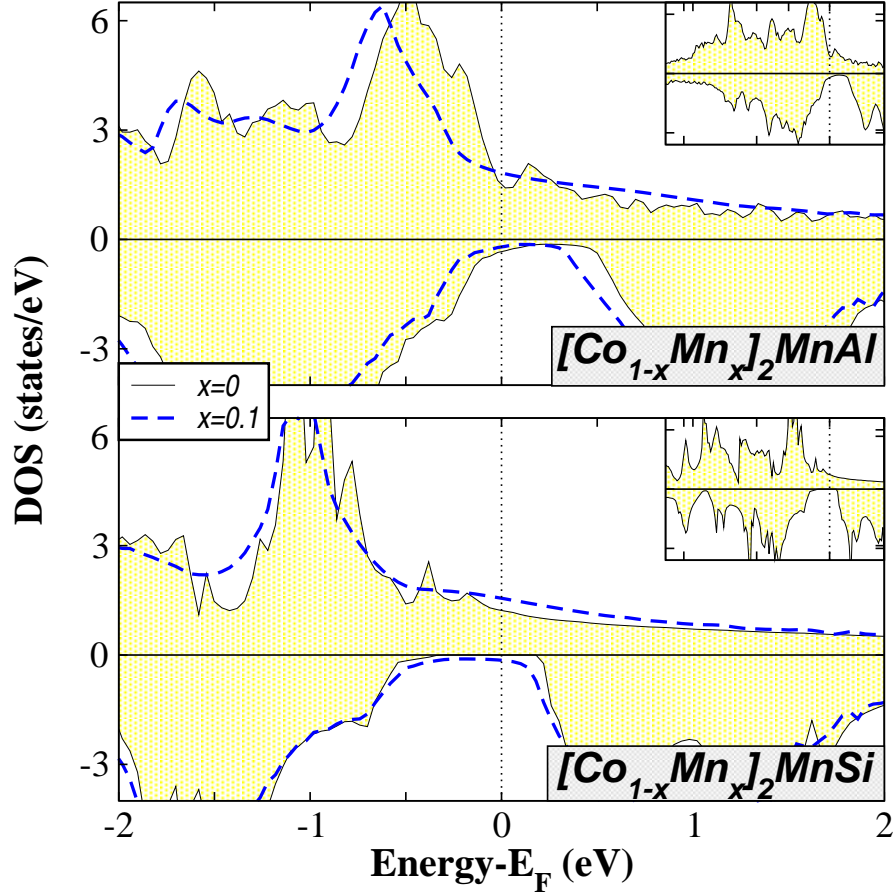


Fig. 4. (Color online) Total density of states (DOS) around the gap region for the $[\text{Co}_{1-x}\text{Mn}_x]_2\text{MnAl}$ and $[\text{Co}_{1-x}\text{Mn}_x]_2\text{MnSi}$ alloys as a function of the concentration x : we denote $x = 0$ with the solid grey line with shaded region and $x = 0.1$ with a dashed thick blue line. In the insets we present the DOS for a wider energy region and for a $x = 0$ concentration.

compound is a perfect half-metal. Co_2MnAl presents in reality a region of tiny minority-spin DOS instead of a real gap, but the spin-polarization at the Fermi level only marginally deviates from the ideal 100% and this alloy can be also considered as half-metal. These results agree with previous electronic structure calculations on these compounds [52, 61, 70, 83, 95]. When we create a surplus of Mn atoms which migrate at sites occupied by Co atoms in the perfect alloys, the gap persists and both compounds retain their half-metallic character as occurs also for the Cr-based alloys presented above. Especially for Co_2MnSi , the creation of Mn antisites does not alter the width of the gap

and the half-metallicity is extremely robust in these alloys with respect to the creation of Mn antisites. The atomic spin moments show behavior similar to the Cr alloys as can be seen in table 2 and the spin moments of the Mn impurity atoms are antiferromagnetically coupled to the spin moments of the Co and Mn atoms at the perfect sites resulting to the desired half-metallic ferrimagnetism.

4 A possible route to half-metallic antiferromagnetism

Now, we will present a way to use the defects in perfect half-metallic ferrimagnets in order to create a half-metallic antiferromagnetic material: the doping with Co of the Mn_2VAl and Mn_2VSi alloys which are well known to be HMF. The importance of this route stems from the existence of Mn_2VAl in the Heusler $L2_1$ phase as shown by several groups [96, 97, 98]. Each Mn atom has a spin moment of around $-1.5 \mu_B$ and V atom a moment of about $0.9 \mu_B$ [96, 97, 98].

All theoretical studies on Mn_2VAl agree on the half-metallic character with a gap at the spin-up band instead of the spin-down band as for the other half-metallic Heusler alloys [52, 76, 99, 100]. Prior to the presentation of our results we have to note that due to the Slater-Pauling rule [52], these compounds with less than 24 valence electrons have negative total spin moments and the gap is located at the spin-up band. Moreover the spin-up electrons correspond to the minority-spin electrons and the spin-down electrons to the majority electrons contrary to the other Heusler alloys [52]. We have substituted Co for Mn in $\text{Mn}_2\text{V}(\text{Al or Si})$ in a random way and in figure 5 we present the total and atom-resolved density of states (DOS) in $[\text{Mn}_{1-x}\text{Co}_x]_2\text{VAl}$ (solid black line) and $[\text{Mn}_{1-x}\text{Co}_x]_2\text{VSi}$ (blue dashed line) alloys for $x=0.1$. The perfect compounds show a region of low spin-up DOS (we will call it a “pseudogap”) instead of a real gap. Upon doping the pseudogap at the spin-up band persists and the quaternary alloys keep the half-metallic character of the perfect Mn_2VAl and Mn_2VSi compounds. Co atoms are strongly polarized by the Mn atoms since they occupy the same sublattice and they form Co-Mn hybrids which afterwards interact with the V and Al or Si states [52]. The spin-up Co states form a common band with the Mn ones and the spin-up DOS for both atoms has similar shape. Mn atoms have less weight in the spin-down band since they accommodate less charge than the heavier Co atoms.

In table 3 we have gathered the total and atom-resolved spin moments for all the Co-doped compounds as a function of the concentration. We have gone up to a concentration which corresponds to 24 valence electrons in the unit cell, thus up to $x=0.5$ for the $[\text{Mn}_{1-x}\text{Co}_x]_2\text{VAl}$ and $x=0.25$ for the $[\text{Mn}_{1-x}\text{Co}_x]_2\text{VSi}$ alloys. In the last column we have included the total spin moment predicted by the Slater-Pauling rule for the perfect half-metals [52]. A comparison between the calculated and ideal total spin moments reveals

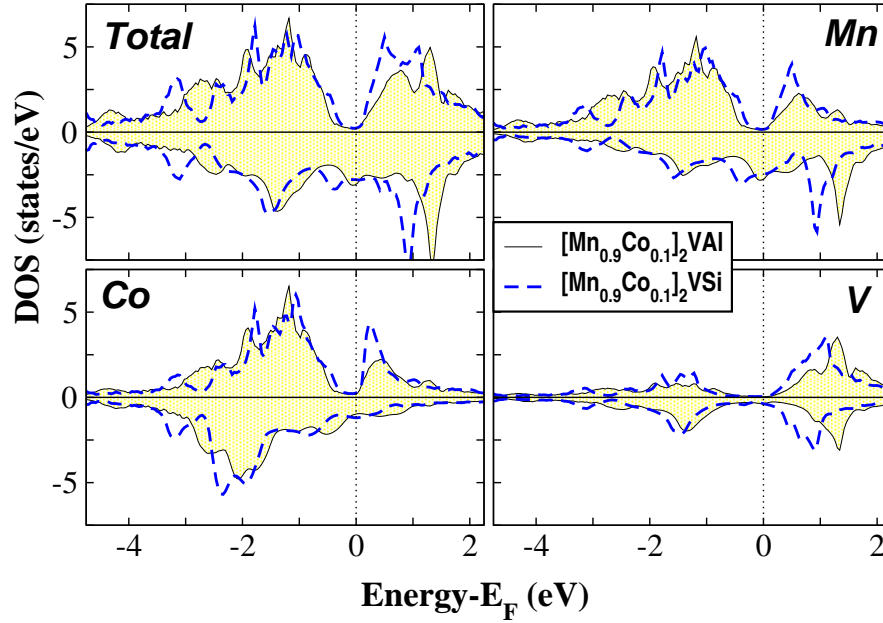


Fig. 5. (Color online) Total and atom-resolved DOS for the $[\text{Mn}_{0.9}\text{Co}_{0.1}]_2\text{VAl}$ and $[\text{Mn}_{0.9}\text{Co}_{0.1}]_2\text{VSi}$ compounds. Note that the atomic DOS's have been scaled to one atom. Positive values of DOS correspond to the spin-up (minority) electrons while negative values correspond to the spin-down (majority) electrons.

that all the compounds under study are half-metals with very small deviations due to the existence of a pseudogap instead of a real gap. Exactly for 24 valence electrons the total spin moment vanishes as we will discuss in the next paragraph. Co atoms have a spin moment parallel to the V one and antiparallel to the Mn moment, and thus the compounds retain their ferrimagnetic character. As we increase the concentration of the Co atoms in the alloys, each Co has more Co atoms as neighbors, it hybridizes stronger with them and its spin moment increases while the spin moment of the Mn atom decreases (these changes are not too drastic). The sp atoms have a spin moment antiparallel to the Mn atoms as already discussed in reference [75].

The most interesting point in this substitution procedure is revealed when we increase the Co concentration to a value corresponding to 24 valence electrons in the unit cell, thus the $[\text{Mn}_{0.5}\text{Co}_{0.5}]_2\text{VAl}$ and $[\text{Mn}_{0.75}\text{Co}_{0.25}]_2\text{VSi}$ alloys. The Slater-Pauling rule predicts for these compounds a zero total spin moment in the unit cell and the electrons population is equally divided between the two spin-bands. Our first-principles calculations reveal that this is actually the case. The interest arises from the fact that although the total moment is zero, these two compounds are made up from

Table 3. Atom-resolved spin magnetic moments for the $[\text{Mn}_{1-x}\text{Co}_x]_2\text{VAl}$ and $[\text{Mn}_{1-x}\text{Co}_x]_2\text{VSi}$ compounds (moments have been scaled to one atom). The two last columns are the total spin moment (Total) in the unit cell calculated as $2 \times [(1-x) * m^{\text{Mn}} + x * m^{\text{Co}}] + m^{\text{V}} + m^{\text{Al or Si}}$ and the ideal total spin moment predicted by the Slater-Pauling rule for half-metals (see reference [52]). The lattice constants have been chosen 0.605 nm for Mn_2VAl and 0.6175 for Mn_2VSi for which both systems are half-metals (see reference [75]) and have been kept constant upon Co doping.

$[\text{Mn}_{1-x}\text{Co}_x]_2\text{VAl}$						
x	Mn	Co	V	Al	Total	Ideal
0	-1.573	—	1.082	0.064	-2.000	-2.0
0.05	-1.580	0.403	1.090	0.073	-1.799	-1.8
0.1	-1.564	0.398	1.067	0.069	-1.600	-1.6
0.3	-1.484	0.456	0.953	0.047	-0.804	-0.8
0.5	-1.388	0.586	0.782	0.019	~0	0
$[\text{Mn}_{1-x}\text{Co}_x]_2\text{VSi}$						
x	Mn	Co	V	Si	Total	Ideal
0	-0.960	—	0.856	0.063	-1.000	-1.0
0.05	-0.944	0.749	0.860	0.059	-0.800	-0.8
0.1	-0.925	0.819	0.847	0.054	-0.600	-0.6
0.2	-0.905	0.907	0.839	0.046	-0.201	-0.2
0.25	-0.899	0.935	0.839	0.041	~0	0

strongly magnetic components. Mn atoms have a mean spin moment of $\sim 1.4 \mu_B$ in $[\text{Mn}_{0.5}\text{Co}_{0.5}]_2\text{VAl}$ and $\sim 0.9 \mu_B$ in $[\text{Mn}_{0.75}\text{Co}_{0.25}]_2\text{VSi}$. Co and V have spin moments antiferromagnetically coupled to the Mn ones which for $[\text{Mn}_{0.5}\text{Co}_{0.5}]_2\text{VAl}$ are ~ 0.6 and $\sim 0.8 \mu_B$, respectively, and for $[\text{Mn}_{0.75}\text{Co}_{0.25}]_2\text{VSi}$ ~ 0.9 and $\sim 0.8 \mu_B$. Thus these two compounds are half-metallic fully-compensated ferrimagnets or as they are best known in literature half-metallic antiferromagnets.

5 Vacancies

Finally we will also shortly discuss a special case: the occurrence of vacancies [88]. In experiments a vacancy can appear in all possible sites and we will start our discussion by the case of vacancies (E) appearing at the sites occupied by Co atoms at the perfect compounds. In figure 6 we have gathered the total density of states (DOS) for the four studied compounds, $[\text{Co}_{1-x}\text{E}_x]_2\text{YZ}$ (Y is Cr or Mn and Z is Al or Si) when we replace 2.5% ($x=0.025$) and 10% ($x=0.10$) of the Co atoms. Although there is no visible effect on the properties of the gap with respect to the perfect compound [83, 86] when x is as small as 0.025, as we increase x to 0.1 impurity states located at the left edge of the gap appear. The vacancy carries very small charge with a vanishing DOS and the induced minority states are mainly located at the Co sites (Mn and

Si atoms have a very small DOS at the same energy range as a result of the polarization of these Co-located vacancy-induced minority-states). These states result in a considerable shrinking of the width of the gap of the order of 0.25-0.3 eV. In the case where the Fermi level is close to the left edge of the gap as in the Co_2MnAl alloy the shrinking of the gap results in the loss of half-metallicity (the spin-polarization is reduced to $\sim 40\%$ for $x = 0.1$).

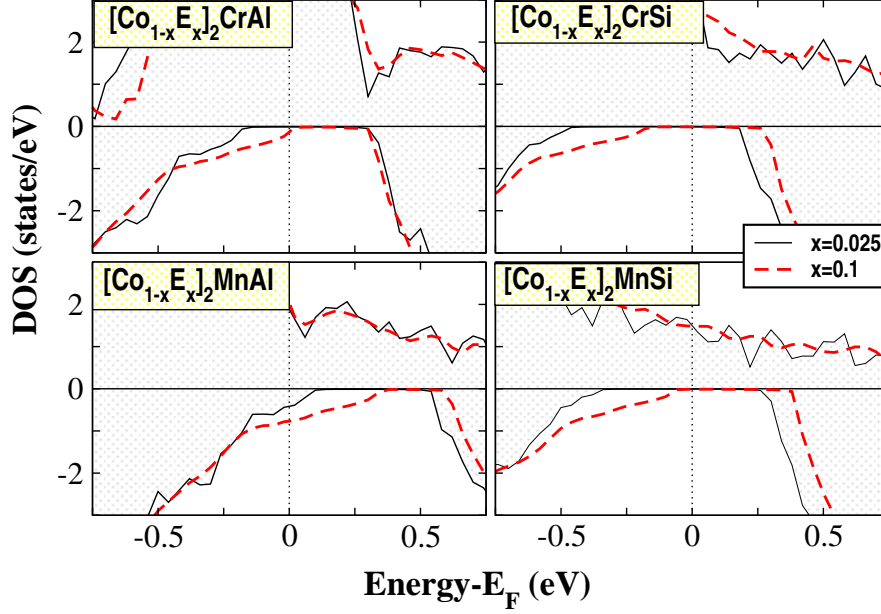


Fig. 6. (Color online) Total density of states (DOS) as a function of the concentration x for the four studied alloys $[\text{Co}_{1-x}\text{E}_{x/2}]_2\text{YZ}$ where Y stands for Cr and Mn, Z for Al and Si and E the vacant site.

In the case when the vacancies occur at the Y site occupied in the perfect alloys by Cr or Mn atoms and the Z site occupied by Al or Si, they again induce minority states within the left edge of the gap leading to a shrinking of its width as in the case discussed in the previous paragraph. But the effect is much more mild leading to a shrinking of the gap by 0.1 eV approximately when they substitute Y-type atoms and even less when they substitute the sp atoms. Moreover, not only the reduction of the width of the gap is smaller, but also the intensity of the minority-spin induced DOS within the gap is smaller with respect to the case discussed in the previous paragraph. This difference in the behavior of the vacancy-induced minority states has its routes to the fact that the gap is created between states exclusively localized at the Co sites which due to symmetry reasons do not couple to Cr(Mn) or Al(Si) orbitals. When the vacancy substitutes Co atoms the effect is much more

intense around the Fermi level than when it substitutes Cr(Mn) or Al(Si) atoms which have almost zero weight around the gap. This is also reflected on the change of the behavior of the atomic spin moments (see reference [88]) for an extended discussion of spin moments).

6 Summary and outlook

In this chapter we have reviewed our results on the defects in half-metallic Heusler alloys. Firstly we have studied the effect of doping and disorder on the magnetic properties of the $\text{Co}_2\text{MnAl}(\text{Si})$ full-Heusler alloys. Doping simulated by the substitution of Cr and Fe for Mn overall keeps the half-metallicity. Both disorder and doping have little effect on the half-metallic properties of Co_2MnSi and it keeps a high degree of spin-polarization. Co_2MnAl presents a region of low minority density of states instead of a real gap. Doping keeps the half-metallicity of Co_2MnAl while disorder simulated by excess of either the Mn or Al atoms completely destroys the almost perfect spin-polarization of the perfect compound contrary to Co_2MnSi .

Afterwards, we have studied the effect of defects-driven appearance of half-metallic ferrimagnetism in the case of the $\text{Co}_2\text{Cr}(\text{Mn})\text{Al}(\text{Si})$ Heusler alloys. More precisely, based on first-principles calculations we have shown that when we create Cr(Mn) antisites at the Co sites, these impurity Cr(Mn) atoms couple antiferromagnetically with the Co and the Cr(Mn) atoms at the perfect sites while keeping the half-metallic character of the parent compounds. This is a promising alternative way to create robust half-metallic ferrimagnets, which are crucial for magnetoelectronic applications. Moreover we have also studied the effect of doping the half-metallic ferrimagnets Mn_2VAl and Mn_2VSi . Co substitution for Mn keeps the half-metallic character of the parent compounds and when the total number of valence electrons reaches the 24, the total spin moment vanishes as predicted by the Slater-Pauling rule and the ideal half-metallic antiferromagnetism is achieved. Thus we can create half-metallic antiferromagnets simply by introducing Co atoms in the Mn_2VAl and Mn_2VSi half-metallic ferrimagnets. Since crystals and films of both Mn_2VAl and Co_2VAl alloys have been grown experimentally, such a compound maybe is feasible experimentally.

Finally, we have studied the effect of vacancies in half-metallic Heusler alloys. We have shown using ab-initio electronic structure calculations that the occurrence of vacancies at the sites occupied by Co atoms in the perfect compounds seriously affects the stability of their half-metallic character and the minority-spin gap is rapidly shrinking. On the other hand vacancies at the other sites do not have an important impact on the electronic properties of the half-metallic full-Heusler compounds. Thus it is crucial for spintronic applications to prevent creation of vacancies during the growth of the half-metallic full-Heusler alloys used as electrodes in the magnetoelectronic devices.

Although we have presented several aspects of defects in Heusler alloys, many more calculations and experiments are needed; the aim is to find systems, which either do not lead to states in the gap (like the defects-driven half-metallic ferrimagnets presented in sections 3 and 4) or systems with particularly high defect formation energies or sufficiently low annealing temperatures (we have not discussed the energetics of defects in this contribution). Equally important for realistic applications is the control of surface and interface states in the gap, the latter are in particular important for interfaces to semiconductors, which we have not been examined in this chapter.

References

1. F. Heusler: Verh. Dtsch. Phys. Ges. **5**, 219 (1903)
2. P.J. Webster and K.R.A. Ziebeck. In: *Alloys and Compounds of d-Elements with Main Group Elements. Part 2.*, Landolt-Börnstein, New Series, Group III, vol 19c, ed by H.R.J. Wijn, (Springer, Berlin 1988) pp 75–184
3. K.R.A. Ziebeck and K.-U. Neumann. In: *Magnetic Properties of Metals*, Landolt-Börnstein, New Series, Group III, vol 32/c, ed by H.R.J. Wijn, (Springer, Berlin 2001) pp 64–414
4. J. Pierre, R.V. Skolozdra, J. Tobola, S. Kaprzyk, C. Hordequin, M.A. Kouacou, I. Karla, R. Currat, and E. Lelièvre-Berna: J. Alloys Comp. **262-263**, 101 (1997)
5. J. Tobola, J. Pierre, S. Kaprzyk, R.V. Skolozdra, and M.A. Kouacou: J. Phys.: Condens. Matter **10**, 1013 (1998)
6. J. Tobola and J. Pierre: J. Alloys Comp. **296**, 243 (2000)
7. J. Tobola, S. Kaprzyk, and P. Pecher: Phys. St. Sol. (b) **236**, 531 (2003)
8. K. Watanabe: Trans. Jpn. Inst. Met. **17**, 220 (1976)
9. R.A. de Groot, F.M. Mueller, P.G. van Engen, and K.H.J. Buschow: Phys. Rev. Lett. **50**, 2024 (1983)
10. Half-metallic alloys: fundamentals and applications, Eds.: I. Galanakis and P. H. Dederichs, Lecture notes in Physics vol. 676 (Berlin Heidelberg: Springer 2005)
11. I. Galanakis, Ph. Mavropoulos, and P. H. Dederichs: J. Phys. D: Appl. Phys. **39**, 765 (2006)
12. I. Galanakis and Ph. Mavropoulos: J. Phys.: Condens. Matter **19**, 315213 (2007)
13. P. H. Dederichs, I. Galanakis, and Ph. Mavropoulos: J. Electron Microscopy **54**, i53 (2005)
14. R.J. Soulen Jr., J.M. Byers, M.S. Osofsky, B. Nadgorny, T. Ambrose, S.F. Cheng, P.R. Broussard, C.T. Tanaka, J. Nowak, J.S. Moodera, A. Barry, and J.M.D. Coey: Science **282**, 85 (1998)
15. H. Kato, T. Okuda, Y. Okimoto, Y. Tomioka, K. Oikawa, T. Kamiyama, and Y. Tokura: Phys. Rev. B **69**, 184412 (2004)
16. T. Shishidou, A.J. Freeman, and R. Asahi: Phys. Rev. B **64**, 180401 (2001)
17. Ph. Mavropoulos and I. Galanakis: J. Phys.: Condens. Matter **19**, 315221 (2007)
18. I. Galanakis: Phys. Rev. B **66**, 012406 (2002)

19. I. Galanakis and Ph. Mavropoulos: Phys. Rev. B **67**, 104417 (2003)
20. Ph. Mavropoulos and I. Galanakis: J. Phys.: Condens. Matter **16**, 4261 (2004)
21. S. Sanvito and N.A. Hill: Phys. Rev. B **62**, 15553 (2000)
22. A. Continenza, S. Picozzi, W.T. Geng, and A.J. Freeman: Phys. Rev. B **64**, 085204 (2001)
23. B.G. Liu: Phys. Rev. B **67**, 172411 (2003)
24. B. Sanyal, L. Bergqvist, and O. Eriksson: Phys. Rev. B **68**, 054417 (2003)
25. W.-H. Xie, B.-G. Liu, and D.G. Pettifor: Phys. Rev. B **68**, 134407 (2003)
26. W.-H. Xie, B.-G. Liu, and D.G. Pettifor: Phys. Rev. Lett. **91**, 037204 (2003)
27. Y.Q. Xu, B.-G. Liu, and D.G. Pettifor: Phys. Rev. B **68**, 184435 (2003)
28. M. Zhang, H. Hu, G. Liu, Y. Cui, Z. Liu, J. Wang, G. Wu, X. Zhang, L. Yan, H. Liu, F. Meng, J. Qu, and Y. Li: J. Phys: Condens. Matter **15**, 5017 (2003)
29. C.Y. Fong, M.C. Qian, J.E. Pask, L.H. Yang, and S. Dag: Appl. Phys. Lett. **84**, 239 (2004)
30. J.E. Pask, L.H. Yang, C.Y. Fong, W.E. Pickett, and S. Dag: Phys. Rev. B **67**, 224420 (2003)
31. J.-C. Zheng and J.W. Davenport: Phys. Rev. B **69**, 144415 (2004)
32. H. Akinaga, T. Manago, and M. Shirai: Jpn. J. Appl. Phys. **39**, L1118 (2000)
33. M. Mizuguchi, H. Akinaga, T. Manago, K. Ono, M. Oshima, and M. Shirai: J. Magn. Magn. Mater. **239**, 269 (2002)
34. M. Mizuguchi, H. Akinaga, T. Manago, K. Ono, M. Oshima, M. Shirai, M. Yuri, H.J. Lin, H.H. Hsieh, and C.T. Chen: J. Appl. Phys. **91**, 7917 (2002)
35. M. Mizuguchi, M. K. Ono, M. Oshima, J. Okabayashi, H. Akinaga, T. Manago, and M. Shirai: Surf. Rev. Lett. **9**, 331 (2002)
36. M. Nagao, M. Shirai, and Y. Miura: J. Appl. Phys. **95**, 6518 (2004)
37. K. Ono, J. Okabayashi, M. Mizuguchi, M. Oshima, A. Fujimori, and H. Akinaga: J. Appl. Phys. **91**, 8088 (2002)
38. M. Shirai: Physica E **10**, 143 (2001)
39. M. Shirai: J. Appl. Phys. **93**, 6844 (2003);
40. J.H. Zhao, F. Matsukura, K. Takamura, E. Abe, D. Chiba, and H. Ohno: Appl. Phys. Lett. **79**, 2776 (2001)
41. J.H. Zhao, F. Matsukura, K. Takamura, E. Abe, D. Chiba, Y. Ohno, K. Ohtani, and H. Ohno: Mat. Sci. Semicond. Proc. **6**, 507 (2003)
42. M. Horne, P. Strange, W.M. Temmerman, Z. Szotek, A. Svane, and H. Winter: J. Phys.: Condens. Matter **16**, 5061 (2004)
43. A. Stroppa, S. Picozzi, A. Continenza, and A. J. Freeman: Phys. Rev. B **68**, 155203 (2003)
44. H. Akai: Phys. Rev. Lett. **81**, 3002 (1998)
45. J.-H. Park, E. Vescovo, H.-J. Kim, C. Kwon, R. Ramesh, and T. Venkatesan: Nature **392**, 794 (1998)
46. S. Datta and B. Das: Appl. Phys. Lett. **56**, 665 (1990)
47. K.A. Kilian and R.H. Victora: J. Appl. Phys. **87**, 7064 (2000)
48. C.T. Tanaka, J. Nowak, and J.S. Moodera: J. Appl. Phys. **86**, 6239 (1999)
49. J.A. Caballero, Y.D. Park, J.R. Childress, J. Bass, W.-C. Chiang, A.C. Reilly, W.P. Pratt Jr., and F. Petroff: J. Vac. Sci. Technol. A **16**, 1801 (1998)
50. C. Hordequin, J.P. Nozières, and J. Pierre: J. Magn. Magn. Mater. **183**, 225 (1998)
51. S. Ishida, S. Fujii, S. Kashiwagi, and S. Asano: J. Phys. Soc. Jpn. **64**, 2152 (1995)

52. I. Galanakis, P. H. Dederichs, and N. Papanikolaou: Phys. Rev. B **66**, 174429 (2002)
53. A. Bergmann, J. Grabis, B. P. Toperverg, V. Leiner, M. Wolff, H. Zabel, and K. Westerholt: Phys. Rev. B **72**, 214403 (2005)
54. J. Grabis, A. Bergmann, A. Nefedov, K. Westerholt, and H. Zabel: Phys. Rev. B **72**, 024437 (2005)
55. J. Grabis, A. Bergmann, A. Nefedov, K. Westerholt, and H. Zabel: Phys. Rev. B **72**, 024438 (2005)
56. S. Kämmerer, A. Thomas, A. Hütten, and G. Reiss: Appl. Phys. Lett. **85**, 79 (2004)
57. J. Schmalhorst, S. Kämmerer, M. Sacher, G. Reiss, A. Hütten, and A. Scholl: Phys. Rev. B **70**, 024426 (2004)
58. Y. Sakuraba, J. Nakata, M. Oogane, H. Kubota, Y. Ando, A. Sakuma, and T. Miyazaki: Jpn. J. Appl. Phys. **44**, L1100 (2005)
59. X. Y. Dong, C. Adelmann, J. Q. Xie, C. J. Palmström, X. Lou, J. Strand, P. A. Crowell, J.-P. Barnes, and A. K. Petford-Long: Appl. Phys. Lett. **86**, 102107 (2005).
60. M. Kallmayer, H. J. Elmers, B. Balke, S. Wurmehl, F. Emmerling, G. H. Fecher and C. Felser: J. Phys. D: Appl. Phys. **39**, 786 (2006)
61. S. Picozzi, A. Continenza, and A. J. Freeman: Phys. Rev. B **69**, 094423 (2004)
62. S. Picozzi and A. J. Freeman: J. Phys.: Condens. Matter **19**, 315215 (2007)
63. I. Galanakis, P. H. Dederichs, and N. Papanikolaou: Phys. Rev. B **66**, 134428 (2002)
64. I. Galanakis: J. Phys.: Condens. Matter **14**, 6329 (2002)
65. I. Galanakis: J. Magn. Magn. Mater. **288**, 411 (2005)
66. M. Ležaić, I. Galanakis, G. Bihlmayer, and S. Blügel: J. Phys.: Condens. Matter **17**, 3121 (2005)
67. I. Galanakis: J. Phys.: Condens. Matter **16**, 8007 (2004)
68. I. Galanakis, M. Ležaić, G. Bihlmayer, and S. Blügel: Phys. Rev. B **71**, 214431 (2005)
69. I. Galanakis: J. Phys.: Condens. Matter **16**, 3089 (2004)
70. K. Özdoğan, B. Aktaş, I. Galanakis, E. Şaşıoğlu: J. Appl. Phys. **101**, 073910 (2007)
71. I. Galanakis: Phys. Rev. B **71**, 012413 (2005)
72. Ph. Mavropoulos, I. Galanakis, V. Popescu, and P. H. Dederichs: J. Phys.: Condens. Matter **16**, S5759 (2004)
73. E. Şaşıoğlu, L. M. Sandratskii, P. Bruno, and I. Galanakis: Phys. Rev. B **72**, 184415 (2005)
74. I. Galanakis, S. Ostanin, M. Alouani, H. Dreyssé, and J. M. Wills: Phys. Rev. B **61**, 599 (2000)
75. K. Özdoğan, I. Galanakis, E. Şaşıoğlu, and B. Aktaş: J. Phys.: Condens. Matter **18**, 2905 (2006)
76. E. Şaşıoğlu, L. M. Sandratskii, and P. Bruno: J. Phys.: Condens. Matter **17**, 995 (2005)
77. I. Galanakis, K. Özdoğan, E. Şaşıoğlu, and B. Aktaş: Phys. Rev. B **75**, 172405 (2007)
78. K. Koepernik and H. Eschrig: Phys. Rev. B **59**, 1743 (1999)
79. K. Koepernik, B. Velicky, R. Hayn, and H. Eschrig: Phys. Rev. B **58**, 6944 (1998)

80. P. Hohenberg and W. Kohn: Phys. Rev. **136**, B864 (1964)
81. W. Kohn and L.J. Sham: Phys. Rev. **140**, A1133 (1965)
82. J.P. Perdew and Y. Wang: Phys. Rev. B **45**, 13244 (1992)
83. I. Galanakis, K. Özdoğan, B. Aktaş, and E. Şaşıoğlu: Appl. Phys. Lett. **89**, 042502 (2006).
84. K. Özdoğan, E. Şaşıoğlu, B. Aktaş, and I. Galanakis: Phys. Rev. B **74**, 172412 (2006).
85. K. Özdoğan, I. Galanakis, E. Şaşıoğlu, and B. Aktaş: Phys. Stat. Sol. (RRL) **1**, 95 (2007).
86. K. Özdoğan, I. Galanakis, E. Şaşıoğlu, and B. Aktaş: Sol. St. Commun. **142**, 492 (2007)
87. I. Galanakis, K. Özdoğan, E. Şaşıoğlu, and B. Aktaş: Phys. Rev. B **75**, 092407 (2007)
88. K. Özdoğan, E. Şaşıoğlu, and I. Galanakis: Phys. Stat. Sol. (RRL) **1**, 184 (2007)
89. I. Galanakis: J. Phys.: Condens. Matter **16**, 3089 (2004)
90. H.M. Kandpal, G.H. Fecher, C. Felser, and G. Schönhausen: Phys. Rev. B **73**, 094422 (2006)
91. S. Wurmehl, G.H. Fecher, H.C. Kandpal, V. Ksenofontov, C. Felser, and H.-J. Lin: Appl. Phys. Lett. **88**, 032503
92. H. van Leuken and R. A. de Groot: Phys. Rev. Lett. **74**, 1171 (1995)
93. R. A. de Groot, A. M. van der Kraan, and K. H. J. Buschow: J. Magn. Magn. Mater. **61**, 330 (1986)
94. Y. Miura, K. Nagao, and M. Shirai: Phys. Rev B **69**, 144413 (2004)
95. M. Sargolzaei, M. Richter, K. Koepernik, I. Opahle, H. Eschrig, and I. Chaplygin: Phys. Rev. B **74**, 224410 (2006)
96. Y. Yoshida, M. Kawakami, and T. Nakamichi: J. Phys. Soc. Jpn. **50**, 2203 (1981)
97. H. Itoh, T. Nakamichi, Y. Yamaguchi and N. Kazama: Trans. Jpn. Inst. Met. **24**, 265 (1983)
98. C. Jiang, M. Venkatesan, and J. M. D. Coey: Sol. St. Commun. **118**, 513 (2001)
99. S. Ishida, S. Asano, and J. Ishida: J. Phys. Soc. Jpn. **53**, 2718 (1984)
100. R. Weht and W. E. Pickett: Phys. Rev. B **60**, 13006 (1999)